Mass transfer in sillimanite-bearing pelitic schists near Rangeley, Maine

CHARLES THOMAS FOSTER, JR.

Department of Earth and Space Sciences, University of California
Los Angeles, California 90024

Abstract

Reactions in pelites from the lower sillimanite zone on Elephant Mountain in the Rangeley-Oquossoc region are of the cation-exchange type involving diffusion among three assemblages in local equilibrium. Sillimanite nucleated preferentially in biotites near garnets and formed segregations containing sillimanite-rich cores and biotite-rich mantles. Chemical potential gradients between the growing sillimanite, the preexisting staurolite, and matrix garnets caused mass transfer which led to the pseudomorphing of staurolite by micas and the growth of garnet at the expense of matrix. Mass transfer between the sillimanite, staurolite, and garnet segregations has been measured and is compatible with a cation-exchange reaction mechanism in a system open to water. The component with the largest mass transfer in a mean molar reference frame is $AlO_{1.5}$ followed in descending order by SiO_2, H_2O, $KO_{0.5}$, FeO, $NaO_{0.5}$, MgO, MnO, TiO_2 and CaO.

Introduction

Several recent contributions (Carmichael, 1969; Eugster, 1970; Fisher, 1970, 1973) have proposed diffusion-controlled reaction mechanisms to explain the development of metamorphic segregations in pelitic rocks. These studies have shown that reaction mechanisms involving diffusion between assemblages in local equilibrium in different parts of the same rock can be used to explain the mass transfer deduced from qualitative examination of the metamorphic textures. In this work, mass transfer between metamorphic segregations has been measured in a mean molar reference frame to determine quantitatively the relative rates of diffusion of ten components in different domains of the same rock. The mass transfer to and from each segregation is then used to quantitatively test the proposed cation-exchange reaction mechanism for mass balance on the scale of a thin section.

Geologic setting

The rocks studied are polymetamorphosed pelitic schists in the southwest quarter of the Rangeley quadrangle and the southeast quarter of the Oquossoc quadrangle in northwest Maine. Work by Guidotti (1970a, 1970b, 1974) and Moench (1966, 1970a, 1970b, 1971) has established that Ordovician and Siluro-Devonian pelitic, quartzo-feldspathic, and calcareous marine sediments in this region have undergone two periods of deformation prior to a regional metamorphism (staurolite–andalusite–biotite), followed by intrusion of flat-lying quartz diorites that produced a contact aureole overprinting the regional metamorphism. Conditions in the aureole ranged from sillimanite grade (650°C, 5 kbar) near the intrusion to garnet grade (500°C, 4 kbar) 1.5 kilometers above the pluton (Guidotti, 1970b; 1974). Since the intrusion and its associated isograds are flat-lying, the horizontal distances between the isograds and the intrusion shown in Figure 1 are about four times the shortest distance between the surfaces.

Because the entire region contained staurolite-bearing assemblages from the regional metamorphism, the thermal gradient imposed by the intrusion caused prograde metamorphism close to the intrusion, produced little change in assemblages in the upper staurolite zone about 500 meters (shortest distance) from the contact, and caused retrograde metamorphism in rocks farther than 500 meters (shortest distance) from the contact.

This paper is concerned with the prograde processes that take place in the lower sillimanite zone during the latest metamorphism. The low-grade boundary of this zone is marked by the disappearance of chlorite and the appearance of sillima-
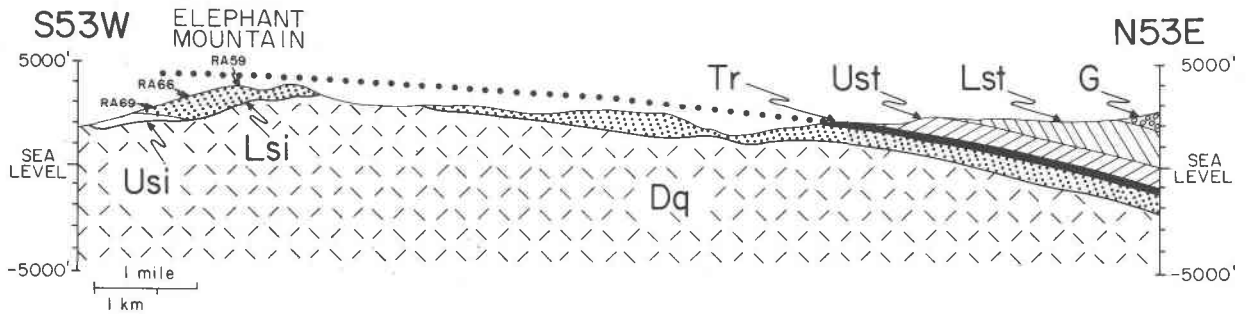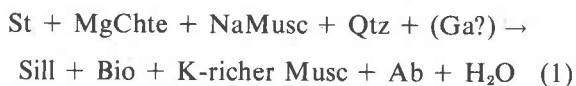
Fig. 1. Cross-section through Elephant Mountain showing the location of outcrops RA59, RA66 and RA69. Isograds are from Guidotti (1970b).

nite via the reaction (Guidotti, 1974);

$$St + MgChte + NaMusc + Qtz + (Ga?) \rightarrow$$

$$Sill + Bio + \text{K-richer Musc} + Ab + H_2O \quad (1)$$

This reaction generally produces less than 1 percent modal sillimanite and uses only trace amounts of staurolite. As grade increases in the lower sillimanite zone, sillimanite grows at the expense of muscovite and biotite, and staurolite is replaced by both micas. These changes have been attributed to the following continuous reaction by Guidotti (1974):

$$MgBio + \text{K,NaMusc} + Ga + MgSt + Qtz \rightarrow$$

$$Sill + FeBio + FeSt$$

$$+ \text{Mn,FeGa} + Ab + H_2O \quad (2)$$
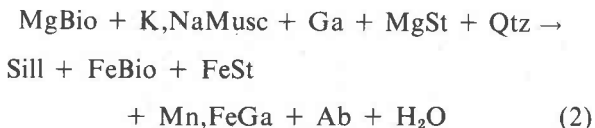
The higher-grade boundary of the lower sillimanite zone is marked by the disappearance of staurolite via the reaction (Guidotti, 1974):

$$St + NaMusc + Qtz \rightarrow Sill + Bio$$

$$+ \text{K-richer Musc} + Ab + Ga + H_2O \quad (3)$$
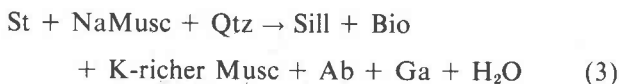
This reaction, like the lower isograd reaction, produces very little sillimanite and consumes only trace amounts of staurolite.

Most of the production of sillimanite and consumption of staurolite in the last metamorphism took place within the lower sillimanite zone. The reaction of staurolite and sillimanite in the last metamorphism was investigated in six hundred specimens collected from seventy large outcrops in Guidotti's (1970b) lower sillimanite zone, between Maine State Highway 17 and the village of South Arm. Thin sections stained for K-feldspar and plagioclase were examined from all localities to determine mineral assemblages and textural relations in rocks of different composition and grade. Because of the flat isograds and high relief, the southwest flank of Elephant

Mountain provides the best cross-section of the lower sillimanite zone. Detailed petrographic and microprobe studies were carried out on fifteen specimens from three outcrops on the mountain to measure the mass transfer involved in reactions between local mineral assemblages within the lower sillimanite zone.

Mineral compositions and textures

Introduction

Staurolite, garnet, biotite, muscovite, plagioclase, and ilmenite were analyzed by microprobe in polished thin section from fifteen specimens which contained the assemblage staurolite + garnet + biotite + muscovite + plagioclase + quartz + sillimanite + ilmenite. The specimens were chosen to show the maximum variation in the degree of replacement of staurolite within each outcrop. The maximum horizontal distance between any of the specimens at an outcrop was 30 meters, and the maximum difference in elevation between any of the specimens at an outcrop was 10 meters. Five of the specimens are from outcrop RA59 at the summit of Elephant Mountain in the low-grade part of the lower sillimanite zone. Six samples are from outcrop RA66 in the middle part of the lower sillimanite zone on the southwest flank of the mountain at 3100 feet. The four highest-grade specimens are from outcrop RA69 near the upper sillimanite/lower sillimanite isograd on the southwest flank at 2500 feet elevation. The relative positions of the outcrops are shown in Figure 1. The modal composition of each rock is given in Figure 2.

Two hundred and eighty total analyses for the RA66 and RA69 specimens were made on the automated MAC microprobe at the Geophysical Laboratory, Carnegie Institute of Washington, using 15 kV accelerating voltage, a five to ten micron beam size and beam currents of 0.025–0.05 microamperes. Data
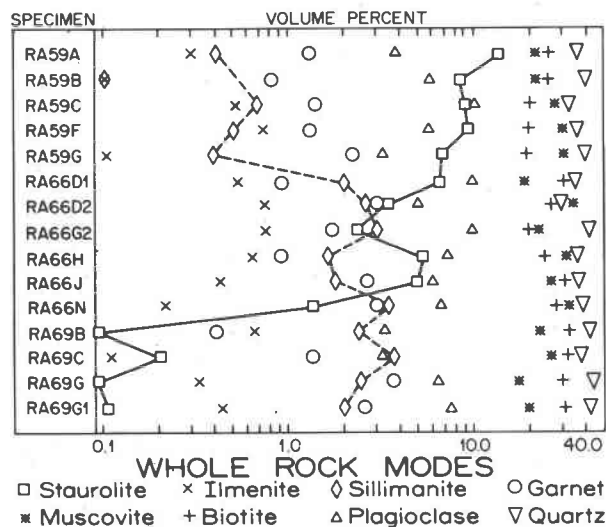
Fig. 2. Whole rock modal compositions for all specimens microprobed; 1000 points counted for each thin section.

were reduced using a Bence-Albee correction scheme. Each analysis is a composite of separate measurements of three to five adjacent regions which were averaged for the final composition.

Ninety total analyses for RA59 specimens and 273 partial analyses for RA66 and RA69 specimens were made on the University of Wisconsin three-channel ARL microprobe with 15 kV accelerating voltage and using a variety of beam size, currents, and counting times to minimize counting times and sample damage. For total analyses, ten to fifteen spots were probed for each analysis, the results averaged and reduced using a Bence-Albee correction scheme to obtain the final value. For partial analyses, the method was similar except that representative "dummy" counts were put in for the elements that were not analyzed for and the results then reduced by Bence and Albee (1968) methods. Molecular formulas were computed by normalizing to the appropriate number of anhydrous oxygens and assuming that an arbitrary amount of H_2O was present. The analytical error on each probe is about 2 percent. Comparison of total analyses of the same grain from the two probes shows that the differences between results from the two probes is ± 2 percent.

Staurolite

Staurolite occurs as poikilitic anhedral to subhedral porphyroblasts in amounts up to sixteen modal percent in high-aluminum specimens from the lowest-grade part of the lower sillimanite zone. It is usually present as five to fifteen millimeter prisms in random orientations, and usually contains about 25 percent poikilitic quartz. The crystallization of staurolite obviously took place after the last tectonic event, because staurolite commonly overprints the spaced cleavage associated with that event by preserving small kink folds shown by the orientation of elongate quartz and mica inclusions. As one proceeds upgrade, staurolite is progressively pseudomorphed by micas texturally different from those in the matrix (Guidotti, 1968). Staurolite ultimately disappears at the lower sillimanite zone/upper sillimanite zone isograd.

Average chemical analyses for staurolites from each specimen are given in Table 1. The formulas were normalized to a unit cell containing 46 anhydrous oxygens. An H_2O content of 2.15 molecules was chosen for this unit cell on the basis of work by Griffen and Ribbe (1973).

Garnet

Garnet occurs as equant anhedral to subhedral porphyroblasts up to 1.5 mm in diameter with poikilitic cores. It generally makes up one to two percent of the rock but can reach up to four percent in the higher-grade rocks near the lower sillimanite zone/upper sillimanite zone isograd. Guidotti (1970a, 1974) has suggested a slight increase in modal garnet as grade increases in the lower sillimanite zone. The same trend was observed in this study, particularly when rocks of similar composition are compared.

Garnet has two distinct morphologies in the lower sillimanite zone. Garnets in or near sillimanite are generally anhedral with deeply embayed rims. Garnets in the matrix or in staurolites tend to be equant with subhedral crystal boundaries and nonpoikilitic rims. In the middle and high-grade portions of the lower sillimanite zone the matrix garnets tend to have larger diameters than the garnets associated with sillimanite. In the lower-grade part of the lower sillimanite zone anhedral garnets are sometimes rimmed by pseudomorphous biotite (Guidotti, 1974).

Average rim and core compositions for garnets from the lower sillimanite zone on Elephant Mountain are summarized in Table 2. Because of complex zoning patterns, the core compositions vary, depending upon the plane of section through the garnet. Note the distinct change in Mn zoning from Mn-rich rims and Mn-poor cores to Mn-rich cores and Mn-poor rims as grade increases on Elephant Mountain. A similar trend has been reported by Guidotti (1974)

Table 1. Average molecular compositions of staurolite. Atoms per anhydrous unit-cell, normalized to 46(O)*

Sample	Mn	Fe	Zn	Mg	Al	Si	Ca	Ti	Sum
RA59A	0.052	3.224	0.038	0.519	17.687	7.815	nd.	nd.	29.335
RA59B	0.049	3.254	0.060	0.497	17.620	7.845	nd.	nd.	29.326
RA59C	0.052	3.180	0.072	0.512	17.736	7.852	nd.	nd.	29.304
RA59F	0.036	3.182	0.044	0.512	17.743	7.802	nd.	nd.	29.319
RA59G	0.037	3.249	0.048	0.496	17.712	7.792	nd.	nd.	29.334
RA66D1	0.042	3.410	0.097	0.471	17.575	7.681	0.000	0.106	29.381
RA66D2	0.024	3.191	0.189	0.427	17.674	7.690	0.000	0.106	29.302
RA66G	0.024	3.115	0.106	0.464	18.079	7.453	0.000	0.106	29.347
RA66H	0.033	3.275	0.109	0.463	17.699	7.641	0.024	0.113	29.357
RA66J	0.033	3.259	0.102	0.455	17.693	7.666	0.000	0.113	29.320
RA66N	0.028	3.204	0.265	0.412	17.577	7.731	0.000	0.104	29.321
RA69B	0.022	2.720	0.693	0.366	17.721	7.732	0.047	0.032	29.333
RA69C	0.028	2.561	0.727	0.291	17.640	7.822	0.023	0.108	29.200
RA69G	0.030	2.539	0.810	0.338	17.640	7.868	0.054	0.000	29.279
RA69G1	0.020	2.748	0.662	0.360	17.588	7.783	0.000	0.114	29.275

* Each unit cell is assumed to contain 2.15 H_2O molecules based on Griffin and Ribbe (1973).

nd. = not determined

between the Oquossoc lower sillimanite zone and the lower-grade Rangeley lower sillimanite zone.

Biotite

Biotite occurs as sub-idioblastic to xenoblastic, red-brown to yellow-brown pleochroic crystals. Three generations of biotites can be distinguished: (1) syntectonic biotites which parallel the penetrative cleavage; (2) post-tectonic biotites that cross-cut the penetrative cleavage in the upper staurolite and lower sillimanite zones, and which apparently grew during the first post-tectonic metamorphism; and (3) biotites that grew in the latest metamorphism, forming a biotite-rich rim around growing sillimanite and replacing staurolite in the mica pseudomorphs after staurolite. Average chemical compositions for biotites from each part of the lower sillimanite zone are given in Table 3. Note that all iron is reported as FeO. No statistically-significant compositional differences were detected between the three generations of biotite.

Muscovite

Muscovite occurs in two distinct habits in the lower sillimanite zone in Rangeley region (Guidotti, 1968). The first type occurs as small thin tablets of oriented muscovite less than 0.5 mm long and 0.1 mm thick, which define the penetrative cleavage produced by the first period of deformation. The second tectonic period folded many of these micas, and they have since been polygonized in the cores of folds by a later metamorphic event. This is the only type of white mica present in the upper staurolite zone and the lowest-grade part of the sillimanite zone. It was clearly produced by an early synkinematic metamorphism and was only slightly modified by later events. The second type of muscovite occurs as large unoriented crystals up to 3 mm long and 1 mm thick which replace staurolite porphyroblasts; they only occur in rocks containing more than 0.1 percent of sillimanite. The random orientation of this mica, plus the fact that it replaces staurolites overprinting the latest cleavage, indicates that this mica is definitely post-kinematic. It is assigned to the latest period of metamorphism because its occurrence is linked to the disappearance of staurolite and growth of sillimanite. Averages of microprobe analyses of muscovite in each specimen are given in Table 4.

Ilmenite

Ilmenite occurs as small anhedral ellipsoids, usually less than 0.1 mm in diameter, which commonly parallel the penetrative cleavage. It is typically present in small amounts (0.5 modal %) in all domains of the rock, but concentrations of up to several percent occur sporadically in the vicinity of sillimanite segregations. Averages of microprobe analyses of ilmenite in each specimen are given in Table 5.

Plagioclase

Plagioclase occurs as weakly zoned, equant, anhedral crystals up to 0.1 mm in diameter which account

Table 2. Average molecular compositions of garnet. Atoms per unit cell, normalized to 12(O)

Sample	Mn	Fe	Zn*	Mg	Al	Si	Ca	Ti	Sum
RA59A									
rim	0.288	2.349	nd.	0.292	2.001	2.993	0.088	0.001	8.012
core	0.275	2.321	nd.	0.304	2.025	2.992	0.076	0.009	8.001
RA59B									
rim	0.273	2.416	0.001	0.249	2.008	2.974	0.096	0.000	8.017
core	0.263	2.364	0.006	0.306	1.993	2.984	0.101	0.001	8.018
RA59C									
rim	0.290	2.323	nd.	0.270	2.013	3.002	0.093	0.001	7.992
core	0.316	2.252	nd.	0.295	2.026	2.993	0.112	0.003	7.997
RA59F									
rim	0.233	2.430	nd.	0.269	2.008	2.984	0.082	0.001	8.007
core	0.231	2.413	nd.	0.266	2.012	2.988	0.095	0.002	8.007
RA59G									
rim	0.215	2.548	nd.	0.285	2.025	3.062	0.078	0.000	8.213
core	0.258	2.467	nd.	0.288	2.031	3.091	0.154	0.006	8.295
RA66D1									
rim	0.236	2.452	0.008	0.257	2.012	2.962	0.079	0.000	8.006
core	0.249	2.399	0.003	0.284	1.999	2.980	0.095	0.000	8.009
RA66D2									
rim	0.199	2.454	0.007	0.254	2.035	2.972	0.081	0.000	8.001
core	0.262	2.403	0.000	0.286	2.025	2.958	0.083	0.000	8.016
RA66G									
rim	0.216	2.395	0.014	0.249	2.041	2.983	0.088	0.000	7.986
core	0.277	2.332	0.010	0.302	2.024	2.970	0.093	0.000	8.008
RA66H									
rim	0.221	2.482	0.011	0.239	2.005	2.974	0.082	0.000	8.014
core	0.262	2.376	0.013	0.285	2.007	2.965	0.113	0.000	8.021
RA66J									
rim	0.206	2.476	0.002	0.244	1.982	3.002	0.088	0.000	8.000
core	0.244	2.385	0.007	0.287	1.998	2.982	0.097	0.000	8.000
RA66N									
rim	0.214	2.475	0.000	0.260	1.993	2.980	0.086	0.000	8.008
core	0.259	2.375	0.000	0.290	1.976	2.991	0.116	0.000	8.008
RA69B									
rim	0.218	2.503	0.017	0.237	2.009	2.957	0.087	0.000	8.028
core	0.247	2.418	0.000	0.249	2.008	2.976	0.107	0.000	8.004
RA69C									
rim	0.211	2.471	0.000	0.230	2.022	2.985	0.077	0.000	7.996
core	0.319	2.313	0.009	0.278	1.999	2.985	0.105	0.000	8.008
RA69G									
rim	0.207	2.472	0.007	0.235	1.990	2.966	0.122	0.013	8.012
core	0.307	2.356	0.000	0.290	1.998	2.970	0.104	0.000	8.025
RA69G1									
rim	0.243	2.475	0.002	0.248	1.992	2.976	0.083	0.000	8.017
core	0.329	2.325	0.009	0.273	2.005	2.969	0.109	0.000	8.021

* *High standard deviations*

for three to eight modal percent of the rock. It is most abundant in the matrix, but is present in all regions of the rock. Weak zoning occurs in plagioclase from all parts of the lower sillimanite zone. Averages of microprobe analyses of the core and rim compositions of plagioclase in each specimen are given in Table 6.

Sillimanite

Sillimanite is present throughout the lower sillimanite zone; it occurs in trace amounts at the bottom of the lower sillimanite zone and increases to a maximum of twelve modal percent at the upper silliman-

ite zone isograd. It generally nucleates and grows epitaxially in biotites, seeming to prefer those biotites that have partially pseudomorphed garnets. As sillimanite becomes more abundant with increasing grade, it replaces the biotite in which it nucleated, forming segregations of fibrolitic sillimanite, quartz, plagioclase, and ilmenite. These segregations tend to grow with their long axes parallel to cleavage, but individual fibrolite crystals within the segregations have random orientations. In the upper part of the lower sillimanite zone the segregations coalesce, forming irregular sillimanite-rich laminations in the

Table 3. Average molecular compositions of biotite. Atoms per anhydrous unit-cell, normalized to 22(0)*

Sample	Mn	Fe**	Zn	Na	Mg	Al	Si	K	Ca	Ti	Sum
RA59A	0.011	2.609	nd.	0.079	1.986	3.546	5.372	1.680	0.000	0.225	15.508
RA59B	0.010	2.703	nd.	0.071	1.935	3.560	5.371	1.660	0.000	0.203	15.515
RA59C	0.010	2.561	nd.	0.070	1.978	3.585	5.394	1.626	0.000	0.220	15.444
RA59F	0.008	2.725	nd.	0.083	1.922	3.559	5.355	1.651	0.000	0.214	15.518
RA59G	0.007	2.800	nd.	0.084	1.893	3.567	5.302	1.636	0.000	0.241	15.530
RA66D1	0.009	2.865	nd.	0.067	1.796	3.555	5.332	1.640	0.000	0.232	15.369
RA66D2	0.009	2.766	nd.	0.061	1.846	3.575	5.346	1.688	0.007	0.206	15.504
RA66G	0.006	2.845	nd.	0.055	1.936	3.519	5.347	1.579	0.000	0.197	15.483
RA66H	0.004	2.742	nd.	0.063	1.812	3.571	5.380	1.664	0.000	0.215	15.452
RA66J	0.013	2.684	nd.	0.082	1.833	3.576	5.356	1.664	0.000	0.254	15.463
RA66N	0.004	2.765	nd.	0.058	1.834	3.514	5.403	1.658	0.000	0.221	15.462
RA69B	0.006	2.845	.nd.	0.074	1.717	3.593	5.383	1.643	0.000	0.194	15.455
RA69C	0.009	2.796	0.016	0.076	1.813	3.584	5.339	1.628	0.000	0.217	15.478
RA69G	0.004	2.843	0.020	0.066	1.745	3.523	5.375	1.676	0.000	0.229	15.481
RA69G1	0.007	2.747	0.005	0.064	1.822	3.563	5.402	1.623	0.000	0.199	15.432

* Each unit cell is assumed to contain 2 H_2O molecules.

** Iron reported as FeO

rock. Above the lower sillimanite zone/upper sillimanite zone isograd, sillimanite needles may occur in all parts of the rock, including the mica pseudomorphs after staurolite. The composition of sillimanite in these specimens was presumed to be Al_2SiO_5. It was not chemically analyzed.

Quartz

Quartz is normally present as equant, weakly-strained anhedral crystals up to 0.5 mm in diameter which make up 20 to 40 percent of the rock by volume. Some of the crystals were polygonized during an early period of deformation. The distribution of quartz in the rock is irregular with some laminations being quartz-rich and others quartz-poor. The com-

position of quartz in these specimens was presumed to be SiO_2. It was not chemically analyzed.

Mineral segregations

In the lowest-grade part of the lower sillimanite zone the rocks contain three distinct compositional regions: sieved staurolite porphyroblasts containing about 20 percent poikilitic quartz; sieved garnet prophyroblasts which are composed of single garnet crystals containing about 10 percent poikilitic quartz in the core; and a matrix containing about 25 percent biotite, 25 percent muscovite, 8 percent plagioclase, less than a percent ilmenite, and 42 percent quartz. Incipient sillimanite segregations are also present, commonly within biotites near garnets.

Table 4. Average molecular compositions of muscovite. Atoms per anhydrous unit-cell, normalized to 22(0)*

Sample	Mn	Fe**	Zn	Na	Mg	Al	Si	K	Ca	Ti	Sum
RA59A	0.002	0.111	nd.	0.324	0.113	5.688	6.224	1.557	0.000	0.042	14.061
RA59B	0.002	0.108	nd.	0.301	0.098	5.658	6.183	1.556	0.000	0.045	13.951
RA59C	0.002	0.101	nd.	0.301	0.098	5.670	6.179	1.527	0.000	0.051	13.929
RA59F	0.002	0.113	nd.	0.338	0.090	5.677	6.172	1.531	0.000	0.042	13.965
RA59G	0.002	0.115	nd.	0.337	0.090	5.707	6.131	1.548	0.000	0.050	13.980
RA66D1	0.000	0.121	nd.	0.311	0.089	5.541	6.207	1.569	0.000	0.054	13.892
RA66D2	0.002	0.127	nd.	0.334	0.085	5.544	6.184	1.596	0.000	0.055	13.927
RA66G	0.000	0.185	nd.	0.308	0.135	5.527	6.162	1.593	0.000	0.051	13.961
RA66H	0.000	0.147	nd.	0.323	0.090	5.563	6.167	1.561	0.000	0.063	13.916
RA66J	0.000	0.123	nd.	0.323	0.098	5.595	6.155	1.588	0.000	0.050	13.932
RA66N	0.000	0.115	nd.	0.323	0.085	5.630	6.146	1.572	0.000	0.050	13.921
RA69B	0.000	0.161	nd.	0.387	0.096	5.605	6.134	1.520	0.000	0.057	13.960
RA69C	0.003	0.135	0.018	0.449	0.074	5.612	6.133	1.520	0.000	0.059	13.945
RA69G	0.000	0.108	0.004	0.330	0.094	5.520	6.223	1.535	0.000	0.056	13.870
RA69G1	0.001	0.122	0.002	0.360	0.099	5.560	6.178	1.523	0.000	0.058	13.903

* Each unit cell is assumed to contain 2 H_2O molecules.

** Iron reported as FeO.

Table 5. Average molecular compositions of ilmenite. Atoms per unit cell, normalized to 6(0)

Sample	Mn	Fe	Zn	Mg	Al	Si	Ti	Sum
RA59A	0.044	1.921	nd.	0.008	nd.	nd.	2.014	3.987
RA59B	0.019	1.930	nd.	0.010	nd.	nd.	2.020	3.979
RA59C	0.048	1.904	nd.	0.008	nd.	nd.	2.020	3.980
RA59F	0.031	1.952	nd.	0.009	nd.	nd.	2.004	3.996
RA59G	0.031	1.931	nd.	0.010	nd.	nd.	2.013	3.985
RA66D1	0.030	1.965	0.011	0.015	0.015	0.035	1.938	4.009
RA66D2	0.027	1.927	0.007	0.007	0.011	0.019	1.997	3.995
RA66G	nd.	2.009	nd.	nd.	nd.	nd.	1.994	4.003
RA66H	0.032	1.931	0.001	0.001	0.006	0.014	2.019	4.004
RA66J	0.031	1.938	0.003	0.000	0.003	0.016	2.021	4.012
RA66N	nd.	1.960	nd.	nd.	nd.	nd.	2.018	3.978
RA69B	0.024	1.982	0.006	0.018	0.012	0.017	1.988	4.056
RA69C	0.025	1.943	0.013	0.010	0.001	0.010	2.013	4.015
RA69G	nd.	1.958	nd.	nd.	nd.	nd.	2.020	3.978
RA69G1	nd.	1.981	nd.	nd.	nd.	nd.	2.007	3.988

With increasing grade the sillimanite grows into lens-shaped bodies several millimeters across containing about 75 percent modal sillimanite and no muscovite. At the same time, a biotite-rich, muscovite-free mantle grows around the sillimanite at the expense of the surrounding matrix. In the upper part of the lower sillimanite zone, the sillimanite segregations have begun to coalesce into biotite-rich, muscovite-free layers parallel to the penetrative cleavage, with sillimanite-rich, muscovite-free regions near the middle of the layer. Eventually these isolated areas of sillimanite unite to form sillimanite laminations within the rock.

After about 0.2 percent modal sillimanite has formed in the rock, staurolite is partially replaced by large micas forming an outer layer separating a central core of poikilitic staurolite from the matrix. The mica rims on staurolite are commonly composed primarily of coarse muscovite, but rarely there is a rim in which coarse biotite predominates. The staurolite/mica boundary is generally deeply embayed, because of the penetration of growing micas into the staurolite core. The mica/matrix boundary is also irregular, but commonly has a gross rectangular cross-section similar to that of a staurolite porphyroblast. Because of the general staurolite-like shape and the presence of isolated trace amounts of staurolite in the outer portions of the mica rims, it is estimated that at least 90 percent of the mica rim forms by replacement of staurolite porphyroblast and less than 10 percent by replacement of matrix. In the upper part of the lower sillimanite zone, the replacement is almost complete; only trace amounts of staurolite remain within large mica pseudomorphs after staurolite.

Garnets in the matrix seem to be growing as grade

increases, because they (1) retain good crystal form, (2) appear to increase in size with grade, (3) are larger than the garnets in the sillimanite segregations, and (4) contain thick nonpoikilitic rims which appear to increase in volume relative to the poikilitic core as grade increases.

In contrast to the garnets growing in the matrix, garnets which seem to have been partially replaced are occasionally present in the sillimanite segregations. These garnets generally show a rather equant crystal form in the biotite portion of the segregation, but are truncated sharply in the sillimanite portion. Most of the replacement of garnet by sillimanite appears to take place at the biotite rim/sillimanite core interface, because garnets in the biotite rim typically display no reaction textures. The total amount of garnet replaced in this manner is probably less than 0.1 modal percent.

The matrix shows essentially no textural changes as grade increases within the lower sillimanite zone. It is characterized primarily by fine-grained white micas oriented parallel to a penetrative cleavage, and somewhat larger biotites which often cross-cut the cleavage. The modes of the core and mantle of the sillimanite segregation, the core and the rim of the staurolite segregation, the matrix around each segregation, and the average matrix are given in Figure 3. Typical

Table 6. Average molecular compositions of plagioclase. Atoms per unit cell, normalized to 8(0)

| Sample		Na	Al	Si	K	Ca	Sum
RA59A	rim	0.743	1.254*	2.746*	0.003	0.254	5.000
	core	0.749	1.248*	2.752*	0.003	0.248	5.000
RA59B	rim	0.760	1.238*	2.762*	0.002	0.238	5.000
	core	0.776	1.245	2.753	0.002	0.220	4.996
RA59C	rim	0.773	1.225*	2.775*	0.002	0.225	5.000
	core	0.772	1.226*	2.774*	0.002	0.226	5.000
RA59F	rim	0.754	1.246*	2.756*	0.002	0.246	5.000
	core	0.764	1.234*	2.766*	0.002	0.234	5.000
RA59G	rim	0.726	1.271*	2.729*	0.003	0.271	5.000
	core	0.719	1.279*	2.721*	0.002	0.279	5.000
RA66D1	rim	0.790	1.208*	2.792*	0.002	0.208	5.000
	core	0.778	1.207*	2.788*	0.002	0.220	5.000
RA66D2	rim	0.803	1.195*	2.805*	0.002	0.195	5.000
	core	0.791	1.207*	2.793*	0.002	0.207	5.000
RA66G	rim	0.788	1.210*	2.790*	0.002	0.210	5.000
	core	0.775	1.233*	2.777*	0.002	0.233	5.000
RA66H	rim	0.790	1.208*	2.792*	0.002	0.208	5.000
	core	0.795	1.203*	2.797*	0.002	0.203	5.000
RA66J	rim	0.790	1.208*	2.792*	0.002	0.208	5.000
	core	0.796	1.202*	2.798*	0.002	0.202	5.000
RA66N	rim	0.769	1.221	2.779	0.002	0.219	5.000
	core	0.787	1.211	2.789	0.002	0.211	5.000
RA69B	rim	0.821	1.203	2.797	0.002	0.176	4.999
	core	0.865	1.204	2.796	0.000	0.135	5.000
RA69C	rim	0.809	1.197	2.805	0.002	0.182	4.995
	core	0.801	1.208	2.793	0.002	0.189	4.993
RA69G	rim	0.838	1.213	2.779	0.003	0.192	5.025
	core	0.799	1.221	2.771	0.003	0.216	5.010
RA69G1	rim	0.775	1.191	2.807	0.003	0.196	4.972
	core	0.810	1.189	2.803	0.003	0.194	4.999

* *Dummy value.*
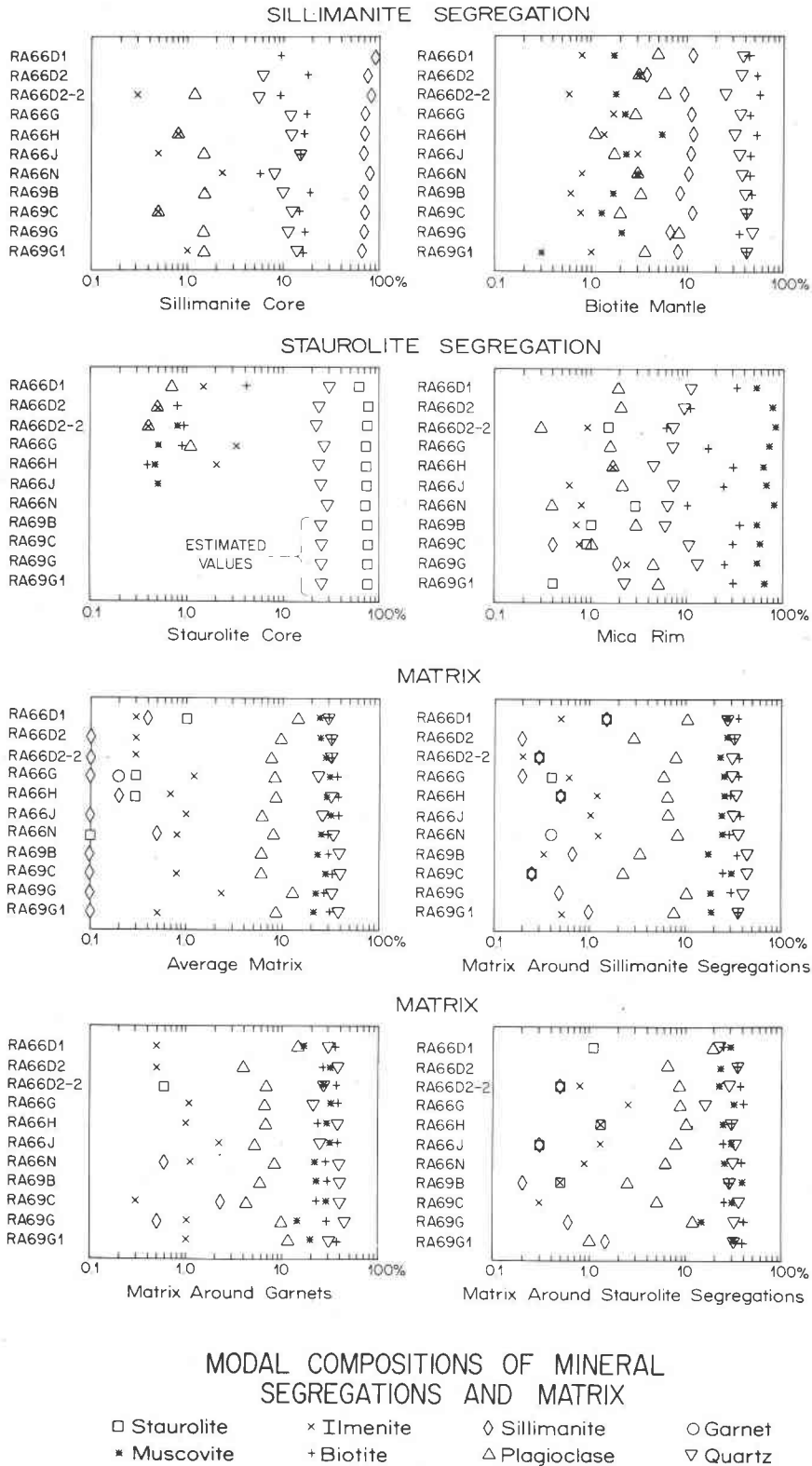
Fig. 3. Modal compositions of mineral segregations; 250 to 400 point counts per region per specimen.

devleopment of the segregations at various grades is shown in Figures 4 and 5.

The three types of segregations (sillimanite, staurolite, and garnet) are distributed throughout the rocks in a fairly uniform manner separated by several millimeters of matrix. Commonly there tends to be a regular one-to-one relationship between a sillimanite segregation, a staurolite segregation, and a matrix garnet, suggesting that the most favorable conditions for growth of a segregation is to have neighboring segregations of the other types in close proximity.

Reaction mechanism

Net reaction

The precise stoichiometric coefficients for the overall reaction among the phases in a rock can be calculated using the principle of the conservation of matter, provided an estimate can be made of the components that enter or leave the system. If matter is conserved, the material lost or gained by the system must equal a linear combination of the compositions of the reacting phases. If the chemical analyses of the phases are error-free, the stoichiometric coefficient of each phase in the reaction may be obtained by: $[\gamma]^{-1}[F] = [S]$ where

$$[\gamma] = \begin{pmatrix} \gamma_{11}\gamma_{12}\cdots\gamma_{1p} \\ \gamma_{21}\gamma_{22}\cdots\gamma_{2p} \\ \cdots \\ \cdots \\ \gamma_{p1}\gamma_{p2}\cdots\gamma_{pp} \end{pmatrix}$$

(γ_{ij} is the number of moles of component i in one mole of phase j. p is the total number of phases present.)

$$[F] = \begin{pmatrix} f_1 \\ f_2 \\ \cdot \\ \cdot \\ \cdot \\ f_p \end{pmatrix}$$

(f_i is the number of moles of component i lost ($+$) or gained ($-$) by the system.)

$$[S] = \begin{pmatrix} s_1 \\ s_2 \\ \cdot \\ \cdot \\ \cdot \\ s_p \end{pmatrix}$$

(s_j is the number of moles of phase j taking part in the reaction.)

and $[\gamma]^{-1}$ is the inverse of $[\gamma]$. If there are more than p independent components in the phases taking part in the reaction, any p of them can be used and will give the same reaction provided the chemical analyses are perfect.

Unfortunately, because this approach balances the reaction exactly, even small analytical errors produce incompatible results when different components are used as basis vectors. To permit the "best fit" of the data using n components, so that the analytical errors tend to balance out, the following matrix equation was used:

$$([\gamma]^T[\gamma])^{-1}[\gamma]^T[F] = [S] \qquad (4)$$

where $[\gamma]$ is now $n \times p$, $[\gamma]^T$ is the $p \times n$ transpose of $[\gamma]$, and $[F]$ is $n \times 1$. This solution results in a least-squares fit of the phase compositions to the known gain or loss of components from the system (Draper and Smith, 1966).

The stoichiometric coefficients for the reaction which would occur if the system was left open to H_2O and closed to all other components were obtained by solving equation (4) using the components MnO, FeO, $NaO_{1.5}$, MgO, $AlO_{1.5}$, SiO_2, $KO_{0.5}$, CaO, TiO_2, and H_2O. ZnO was excluded from the calculation because it tends to remain in the staurolite as the reaction proceeds, merely increasing the ZnO content of staurolite. The γ_{ij} were obtained from the chemical analyses given in Table 1 through 6, and the presumed compositions of sillimanite (Al_2SiO_5) and quartz (SiO_2). Rim compositions were used for garnet and plagioclase. Since the system is closed to all components but water, the f_i are all zero except for the value for water which was chosen to be one so that the calculated reaction is normalized to one mole of H_2O lost from the system. The reaction calculated
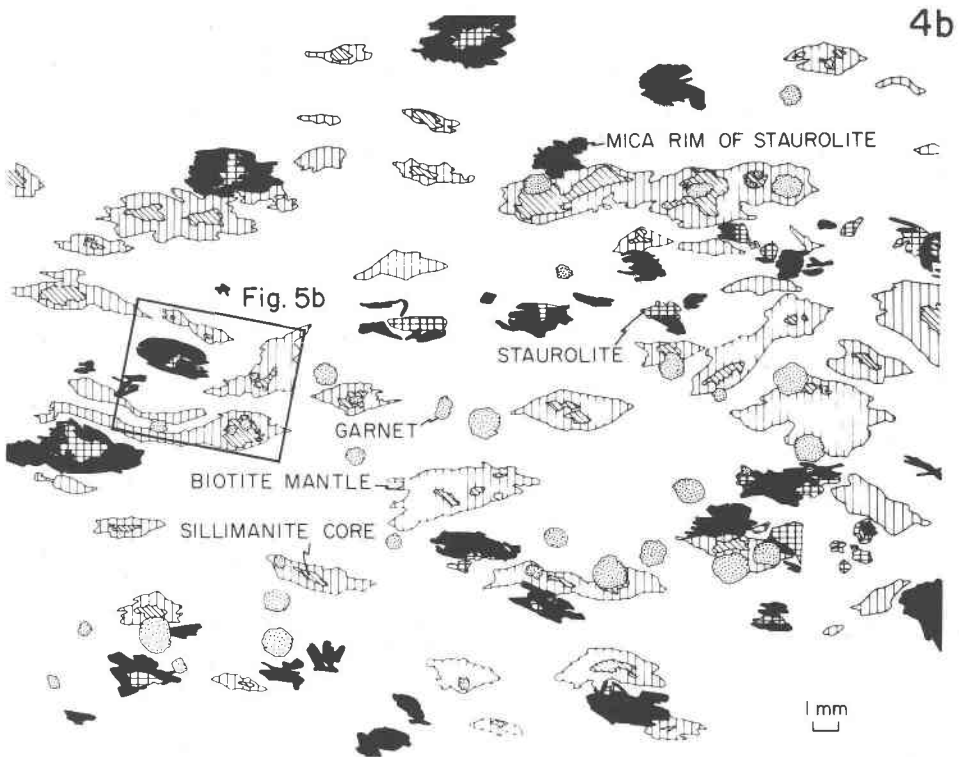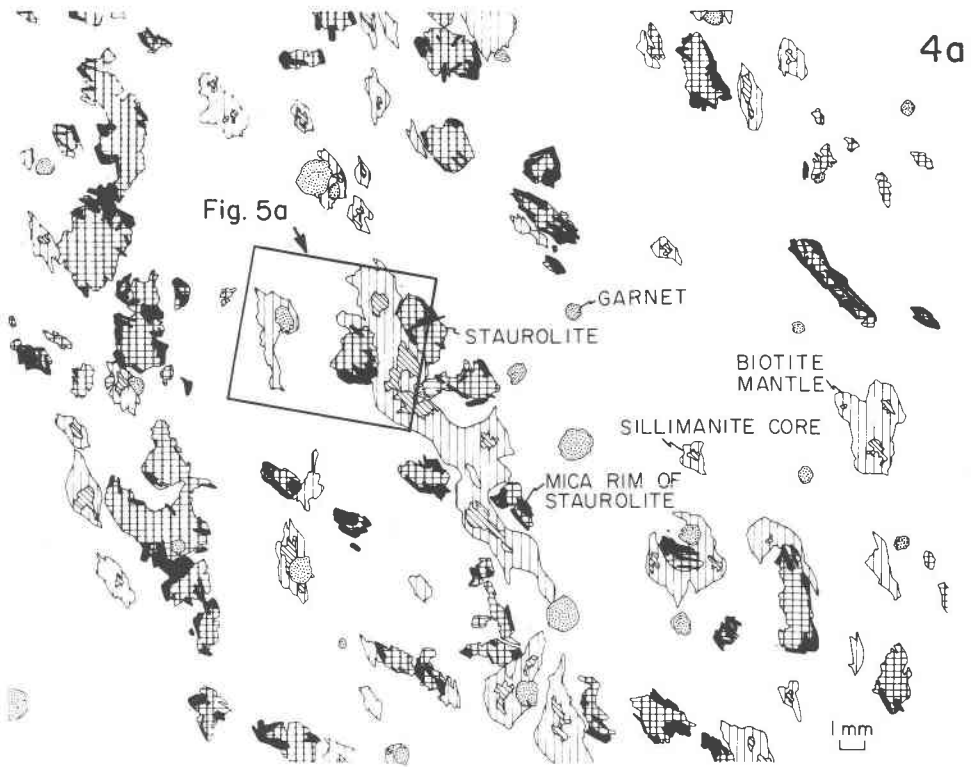
Fig. 4. Sketches of various stages of segregation growth: (a) early stage, (b) intermediate stage, (c) advanced stage. Boxes identify regions shown in Figure 5.
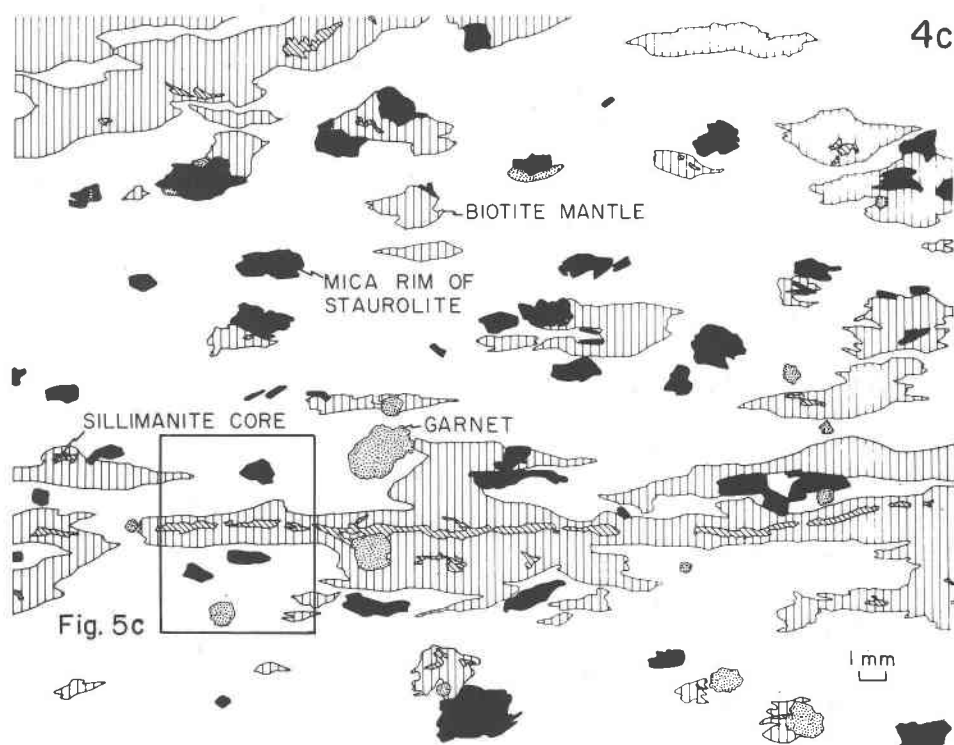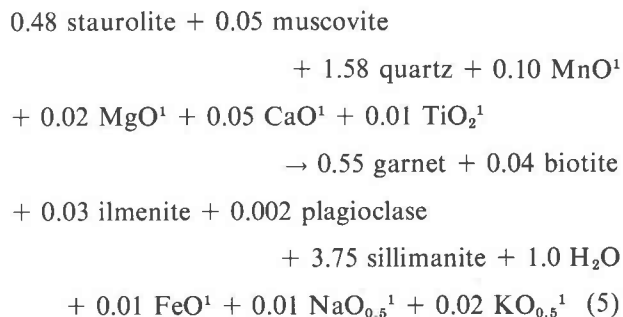
Fig. 4. continued

by this method for a typical specimen (RA66N) is:

0.48 staurolite + 0.05 muscovite

$$+ 1.58 \text{ quartz} + 0.10 \text{ MnO}[1]$$

$$+ 0.02 \text{ MgO}[1] + 0.05 \text{ CaO}[1] + 0.01 \text{ TiO}_2[1]$$

$$\rightarrow 0.55 \text{ garnet} + 0.04 \text{ biotite}$$

$$+ 0.03 \text{ ilmenite} + 0.002 \text{ plagioclase}$$

$$+ 3.75 \text{ sillimanite} + 1.0 \text{ H}_2\text{O}$$

$$+ 0.01 \text{ FeO}[1] + 0.01 \text{ NaO}_{0.5}[1] + 0.02 \text{ KO}_{0.5}[1] \quad (5)$$

The residual components left over or used up by reaction (5) are on the proper side to account for the observed decrease in Mg/Fe and Mn/Fe in biotite, staurolite, and garnet as grade increases in the Oquossoc area (Guidotti, 1974). Thus, the residuals may be due to incongruent reactions occurring among the minerals.

To permit the calculated reaction to be quantitatively verified against observations from the rock, the stoichiometric coefficients of the solid phases were multiplied by molar volumes of the appropriate mineral to give volume coefficients for the reaction.

The molar volumes used for all phases except staurolite are from Robie *et al.* (1966). The value for staurolite is from Griffen and Ribbe (1973). Thermal expansion, compressibility, and compositional corrections were neglected. The volume coefficients were then normalized to the sillimanite volume produced by dividing by the sillimanite volume coefficient. Normalized volume coefficients for all specimens are given in Table 7. The average volume change in the reactions given in Table 7 is $0.0041 \pm 0.0063[2]$ cc per cc of sillimanite produced. Thus, the proposed net reaction essentially conserves volume, even though no constraint was placed on volume in the calculation. Textural evidence suggests volume may also have been conserved locally in the rock, because preexisting foliations and laminations in the matrix near segregations do not appear to have been reoriented during segregation growth.

The amount of staurolite consumed by the sillimanite-forming reaction in each specimen can be computed by multiplying the normalized volume coefficient of staurolite from Table 7 by the modal amount of sillimanite in the rock given in Figure 2. This gives the modal percent of the *phase* staurolite

[1] Residual value left over after least-squares fit.
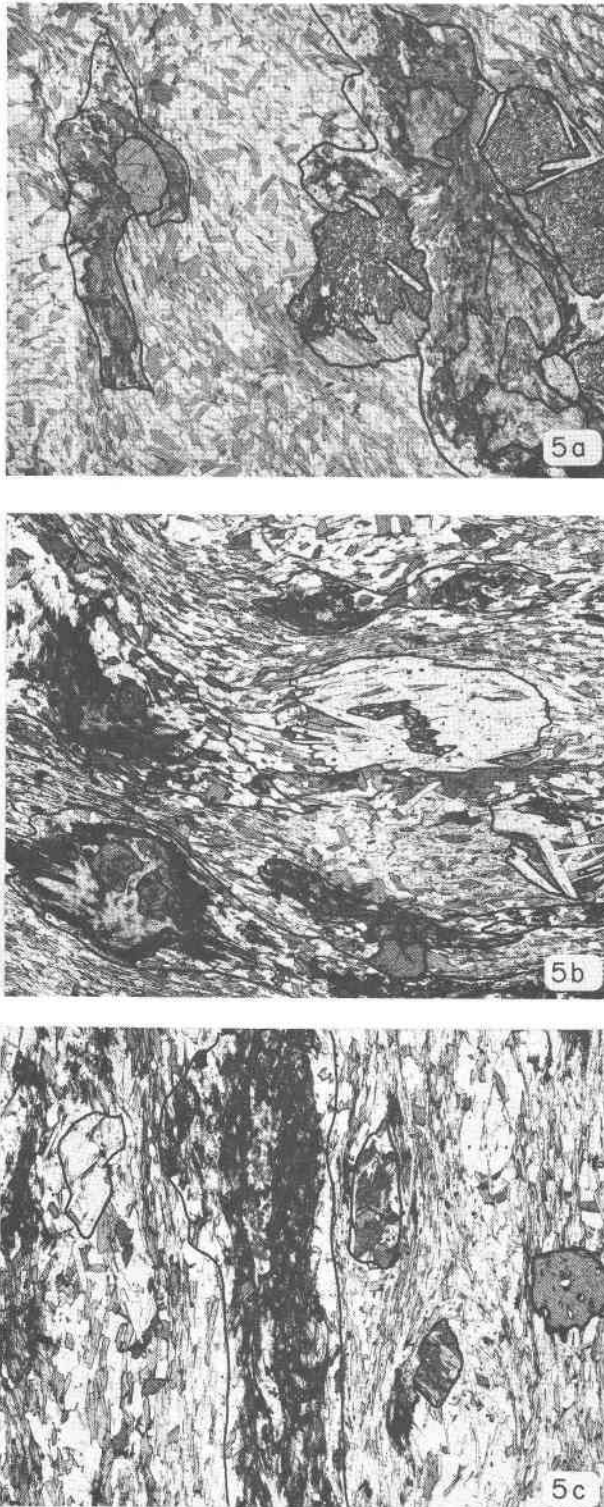
[2] One standard deviation

Fig. 5. Photomicrographs of segregations in various stages of development: (a) early stage, (b) intermediate stage, (c) advanced stage. See Fig. 4 for identification of outlined segregations.

consumed in the sillimanite-forming reaction. This value was then divided by the average volume fraction of staurolite in the remaining porphyroblasts in the specimen (see staurolite core plot in Fig. 3) to obtain the calculated volume percent of poikilitic staurolite *porphyroblasts* consumed in the sillimanite-forming reaction. An independent check on this value is provided by the volume percent of pseudomorphous mica in the rock, which is believed to closely represent the volume of the staurolite porphyroblasts consumed because of its general staurolite-like shape, the presence of small blebs of staurolite near the outer margins of the pseudomorphs, and the lack of reorientation of older matrix foliations in the vicinity of the pseudomorphs, which would accompany a large volume change. If the calculated reaction is correct, the calculated volume of the staurolite porphyroblasts consumed should be close to the amount of pseudomorphous mica in the rock. The volume of dissolved poikilitic staurolite porphyroblasts in each specimen, calculated for a system open to water and ignoring ZnO, are compared with the pseudomorphous mica rim volumes in Table 8. They agree quite well.

Staurolite volume changes calculated for a completely closed system (including H_2O) are approximately twice as large as the amount of pseudomorphous muscovite in the rock. This would require half of a staurolite porphyroblast to be replaced by ordinary-looking matrix if volume is conserved. This is clearly incorrect, because the matrix micas are of an older generation. Therefore, a system closed to water appears to be inconsistent with the nature of the rock, while the net reaction calculated with the system open to H_2O seems to be in agreement with limitations imposed by the texture of the rocks.

Local reactions

The overall reaction discussed above is actually the sum of five local cation-exchange reactions which form mineral segregations in three different regions of the rock. Each "local" region is an open chemical system free to communicate with its neighbors over distances up to a few centimeters via diffusion along grain boundaries in response to chemical potential gradients.

A description of local reactions can take on many different forms, depending upon the reference frame chosen. However, the net amount of each phase used or produced will remain unchanged, no matter what reference frame is chosen (Fisher, 1975). A useful reference frame for diffusion in these rocks is a mean

Table 7. Calculated volume coefficients for reaction in a system closed to all components except H_2O. Volumes produced ($+$) or consumed ($-$) per unit volume of sillimanite produced

Sample	St	Ga	Bio	Musc	I	Plag	Sill	Qtz
RA59A	-1.127	0.3473	0.1109	-0.1422	0.0012	0.0106	1.000	-0.1918
RA59B	-1.115	0.3150	0.1346	-0.1508	0.0105	0.0063	1.000	-0.1863
RA59C	-1.131	0.3515	0.1088	-0.1416	0.0105	0.0104	1.000	-0.1910
RA59F	-1.118	0.3237	0.1205	-0.1378	-0.0006	0.0124	1.000	-0.1886
RA59G	-1.130	0.3316	0.0987	-0.1106	-0.0004	0.0068	1.000	-0.1951
RA66D1	-1.150	0.3577	0.0947	-0.1103	0.0097	0.0047	1.000	-0.1991
RA66D2	-1.143	0.3390	0.0747	-0.0832	0.0091	0.0035	1.000	-0.1957
RA66G	-1.105	0.3145	0.0947	-0.1006	0.0092	0.0037	1.000	-0.2096
RA66H	-1.134	0.3364	0.0842	-0.0976	0.0099	0.0040	1.000	-0.1963
RA66J	-1.131	0.3341	0.0936	-0.1028	0.0087	0.0034	1.000	-0.1986
RA66N	-1.145	0.3400	0.0676	-0.0803	0.0093	0.0012	1.000	-0.1915
RA69B	-1.108	0.2711	0.0804	-0.0908	0.0030	0.0110	1.000	-0.1705
RA69C	-1.119	0.2664	0.0465	-0.0537	0.0091	0.0055	1.000	-0.1608
RA69G	-1.110	0.2594	0.0745	-0.0817	0.0001	0.0061	1.000	-0.1542
RA69G1	-1.116	0.2735	0.0737	-0.0865	0.0102	0.0057	1.000	-0.1627

molar (Brady, 1975) reference frame defined by the relation:

$$\sum_{i=1}^{n} \mathbf{J}_i = 0$$

where $\mathbf{J}_i$ is the flux of component i with respect to a mean molar frame in a system of n components. Fisher (1975) has pointed out that the local reactions depend upon the choice of reference frame for the fluxes, because of the conservation equation. In the mean molar reference frame, this principle requires the local reactions to obey the relationship $\sum_{i=1}^{n} \gamma i = 0$, where γ_i is the stoichiometric coefficient of component i in the local reaction. The components used in this treatment MnO, FeO, ZnO, $NaO_{0.5}$, MgO, $AlO_{1.5}$, SiO_2, $KO_{0.5}$, CaO, TiO_2 and H_2O. Thus, the

sum of H_2O and metal cations is conserved in this reference frame. The local reactions at each interface in a mean molar reference frame may be obtained as follows: (1) Calculate the number of formula units of each phase in each zone from the modal analyses. (2) Normalize the number of formula units of the phases in each zone so that the total amount of *components* in each zone is equal to 1 mole. (3) Subtract the number of normalized formula units of each phase in the reaction zone from the number of normalized formula units of the same phase in the product zone; this gives the reaction at the zone boundary required to convert 1 mole of *components* in the reaction zone to 1 mole of *components* in the product zone. (4) Multiply the reaction so obtained by the number of moles of *components* in the product zone of the segre-

Table 8. Net volume changes in segregations during metamorphism (expressed as volume percent of the whole rock)

Region	66D1	66D2	66D2-2	66G	66H	66J	66N	69B	69C	69G	69G1
				SILLIMANITE SEGREGATION							
Sillimanite core*	0.72%	2.90%	4.10%	2.70%	0.70%	0.97%	1.72%	0.85%	1.10%	1.08%	0.97%
Biotite rim*	7.02%	11.06%	10.40%	12.60%	8.10%	7.42%	11.35%	23.45%	20.29%	21.07%	16.76%
				STAUROLITE SEGREGATION							
Staurolite core**	-3.47%	-4.18%	-4.14%	-5.14%	-2.55%	-2.60%	-5.14%	-3.74%	-4.75%	-3.43%	-2.87%
Mica rim*	3.51%	4.10%	4.02%	5.20%	2.77%	3.00%	5.36%	3.28%	4.92%	3.42%	2.23%
				MATRIX GARNET SEGREGATION							
Garnet**	0.67%	0.92%	0.92%	1.04%	0.54%	0.56%	1.19%	0.69%	0.85%	0.60%	0.53%

* Measured in rock using drawings of thin-sections and a planimeter.

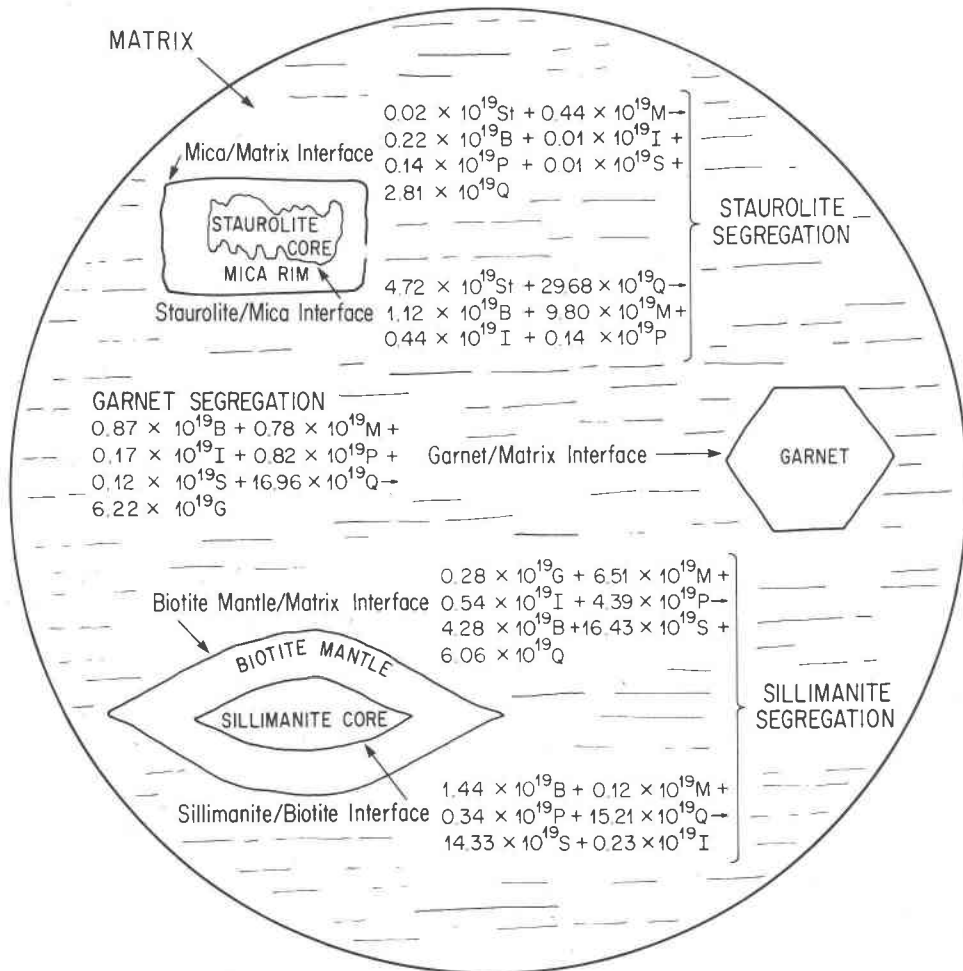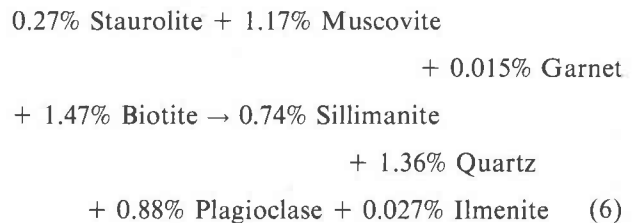** Calculated from volume coefficients in Table 7.

Fig. 6. Coupled local reactions in 10 mm³ of whole rock for specimen RA66N in a mean molar reference frame.

gation;[3] this gives the total reaction at each interface due to the growth of the segregation.

The local reactions at each reacting interface in a mean molar reference frame are shown in Figure 6 for a typical specimen (RA66N). In this reference frame the mica/matrix interface appears to move towards the staurolite core because of the high cation density of the staurolite relative to the mica rim. This does not invalidate the assumption that this boundary represents the original staurolite/matrix boundary position in the rock, because the observations on which the assumption is based are only valid with respect to a volume-fixed reference frame.

The sum of the "local" reactions closely matches the calculated net reaction for the process. The difference between the two reactions can be resolved if the following reaction (in volume percent of the rock) was missed when the local reactions were determined for RA66N:

0.27% Staurolite + 1.17% Muscovite

$$+ \; 0.015\% \; \text{Garnet}$$

$+ \; 1.47\% \; \text{Biotite} \rightarrow 0.74\% \; \text{Sillimanite}$

$$+ \; 1.36\% \; \text{Quartz}$$

$+ \; 0.88\% \; \text{Plagioclase} + 0.027\% \; \text{Ilmenite} \quad (6)$

Reaction (6) is the result of several effects, including small measurement errors in the volumes and modal compositions of the segregations, leakage of components out of the plane of the thin section, and a

---

[3] This number is obtained from the volume changes given in Table 8 using molar volumes from Robie *et al.* (1966) and Griffen and Ribbe (1973), phase compositions from Tables 1 through 6, and modes from Figure 3.

small amount of reaction among the matrix minerals as they buffer the chemical potentials along the diffusion path between segregations.

Mass transfer

The local reactions shown in Figure 6 are not isochemical, requiring that some components must be supplied to the reaction interface while other components must be removed from the reaction interface. Since the modal compositions of the segregations do not seem to show consistent variation between segregation boundaries, nor changes as the reactions proceed (Fig. 3), all the reactions occurring in the rocks are assumed to take place at the boundaries of the segregation zones. If the composition of the grain-boundary phase (fluid?) remains constant at a reaction interface during the reaction, the components produced or consumed must be removed or supplied by diffusion through the regions on either side of the interface. To calculate the amount of each component supplied to or removed from a reaction interface when the grain-boundary phase composition at the interface is constant, the following procedure was used:

(1) The mole fraction of each component in the product region and reactant region was calculated from the modes of each region (from Fig. 3), the mineral compositions (from Tables 1–6), and unit-cell volumes of the minerals (from Robie *et al.,* 1966; Griffen and Ribbe, 1973).

(2) The mole fractions of the product region are subtracted from the reactant region to obtain the amount produced ($+$) or consumed ($-$) per mole of components converted to product region in a mean molar reference frame.

Table 9 gives the average amount of each component consumed or produced by a reaction at each interface during the conversion of solid phases containing one mole of components from reactant to product region. The values in Table 9 were computed by calculating the amount of each component consumed or produced in each specimen according to the procedure outlined in (1) and (2) above, and then calculating the mean and standard deviation(s) for an outcrop using the values for each specimen from the outcrop.

The data presented in Table 9 provide no information about the *total* production or consumption of a

Table 9. Amount (in moles) of each component consumed ($-$) or produced ($+$) by reaction at each interface during conversion of solid phases containing one mole of components from reactant region to product region

Outcrop		MnO	FeO	ZnO	$NaO_{1/2}$	MgO	$AlO_{3/2}$	SiO_2	$KO_{1/2}$	CaO	TiO_2	H_2O
				SILLIMANITE	CORE/BIOTITE	MANTLE	INTERFACE					
RA66	Mean	0.0002	0.0627	0.0000	0.0057	0.0393	−0.3315	0.1314	0.0375	0.0011	0.0082	0.0454
	σ	±0.0001	±0.0057	±0.0000	±0.0025	±0.0042	±0.0831	±0.0730	±0.0049	±0.0007	±0.0075	±0.0054
RA69	Mean	0.0002	0.0523	0.0002	0.0066	0.0323	−0.3458	0.1793	0.0309	0.0011	0.0053	0.0376
	σ	±0.0001	±0.0102	±0.0002	±0.0038	±0.0067	±0.0121	±0.0361	±0.0047	±0.0010	±0.0019	±0.0061
				BIOTITE	MANTLE/MATRIX	INTERFACE						
RA66	Mean	−0.0001	−0.0256	0.0000	0.0102	−0.0154	−0.0044	0.0138	0.0101	0.0015	−0.0039	0.0138
	σ	±0.0001	±0.0083	±0.0000	±0.0030	±0.0065	±0.0192	±0.0388	±0.0057	±0.0009	±0.0049	±0.0070
RA69	Mean	−0.0001	−0.0207	0.0001	0.0070	−0.0117	−0.0056	0.0119	0.0089	0.0006	−0.0031	0.0127
	σ	±0.0001	±0.0113	±0.0001	±0.0027	±0.0066	±0.0144	±0.0346	±0.0027	±0.0007	±0.0024	±0.0034
				GARNET/MATRIX	INTERFACE							
RA66	Mean	−0.0265	−0.2436	0.0000	0.0194	0.0057	−0.0556	0.1607	0.0623	−0.0081	0.0089	0.0167
	σ	±0.0019	±0.0095	±0.0000	±0.0044	±0.0065	±0.0160	±0.0447	±0.0078	±0.0035	±0.0026	±0.0097
RA69	Mean	−0.0272	−0.2518	0.0003	0.0196	0.0056	−0.0752	0.2073	0.0539	−0.0084	0.0084	0.0675
	σ	±0.0020	±0.0085	±0.0003	±0.0037	±0.0039	±0.0039	±0.0285	±0.0043	±0.0019	±0.0034	±0.0061
				MICA	RIM/STAUROLITE	CORE	INTERFACE					
RA66	Mean	0.0007	0.0466	0.0038	−0.0169	−0.0113	0.1532	−0.0239	−0.0887	−0.0001	−0.0028	−0.0605
	σ	±0.0001	±0.0153	±0.0016	±0.0023	±0.0099	±0.0079	±0.0226	±0.0037	±0.0008	±0.0057	±0.0025
RA69	Mean	0.0005	0.0097	0.0186	−0.0198	−0.0259	0.1869	−0.0213	−0.0840	−0.0003	−0.0095	−0.0548
	σ	±0.0002	±0.0071	±0.0017	±0.0018	±0.0044	±0.0127	±0.0215	±0.0048	±0.0011	±0.0067	±0.0068
				MATRIX/MICA	RIM	INTERFACE						
RA66	Mean	−0.0001	−0.0190	0.0000	−0.0037	−0.0133	0.0864	−0.1033	0.0242	−0.0030	0.0006	0.0313
	σ	±0.0001	±0.0245	±0.0001	±0.0092	±0.0152	±0.0459	±0.0493	±0.0104	±0.0023	±0.0055	±0.0134
RA69	Mean	0.0000	−0.0016	0.0002	0.0029	−0.0036	0.0808	−0.1306	0.0205	−0.0008	0.0045	0.0272
	σ	±0.0001	±0.0118	±0.0003	±0.0070	±0.0094	±0.0153	±0.0182	±0.0027	±0.0019	±0.0054	±0.0040

* σ *is one standard deviation*

component at the interfaces, but they do permit comparison of the relative production of components at the same type of interface at different grades. The relative production or consumption of major components at the same type of interface in different specimens is quite similar throughout the entire range of composition and grade represented. This suggests that the reaction mechanisms were relatively insensitive to limited variations in grade and bulk composition, even though mineral compositions are affected.

A more complete description of the mass transfer in a rock during metamorphism can be obtained by normalizing the total number of moles of components produced or consumed by each type of local reaction in a rock since the reaction began to the value expected, if a standard 1 cm³ of rock containing all three types of segregations was considered. This is done by using the formula: $p_i = n/V \cdot \bar{p}_i$; p_i is the amount of component i produced at a particular type of interface per cm³ of whole rock, V is the total volume (in cm³) of the rock under consideration, n is the total number of moles of components converted from reactants to products at the type of interface in question throughout the rock during the metamorphism,[4] and $\bar{p}_i$ is the amount of component i produced by the conversion of one mole of reactants to products. The components produced or consumed by local reactions in 1 cm³ of rock can be examined quantitatively by referring to the mass transfer occurring in a simplified system shown in Figure 7. In Figure 7 each segregation is located at the end of a pipe which is linked to the other segregations by pipes containing matrix material. The total volume of the system is 1

---

[4] n is calculated using the procedure outlined in footnote 3.

Fig. 7. Schematic representation of diffusion system in rock.

cm³. The volume of each segregation is equal to the combined volumes of the segregations of that type present in an average 1 cm³ of the rock in question.

The segregations of Figure 7 communicate with each other by diffusion in the pipes containing matrix material. Components which move towards the center of the system (away from the segregation) are assigned a positive value of mass transfer, while those that move towards segregations have a negative value. The mass transfer in the system was calculated by computing the net amount of components produced or consumed at the interface nearest the end of each pipe in Figure 7. This material must have been supplied or removed by mass transfer in the biotite rim for the sillimanite/biotite interface, in the mica pseudomorph for the staurolite/mica interface, and in the matrix for the garnet/matrix interface, because no reactions are occurring in the sillimanite, staurolite, or garnet regions at the end of the pipes. The mass production for the outermost interfaces of the sillimanite and staurolite segregations was added to the mass transfer in the rim zones of the segregations to obtain the mass transfer in the matrix outside of those segregations.

The mean values of mass transfer for each outcrop obtained by averaging the results of this procedure for each rock at the outcrop are given in Table 10. The magnitudes of the mass transfer in Table 10 depend upon how much segregation growth has occurred in an average 1 cm³ of rock during metamorphism. This is a function of how fast the segregations have been growing (primarily a function of grade) and how many segregations there are per unit volume (primarily a function of bulk composition).

Mass balance

The sum of the mass transfer of each component through the matrix surrounding each segregation is given at the bottom of Table 10. If all the reactions occurring in the rock have been taken into account and the system is closed to all components but water, the sum of the mass transfer should be zero for all components except water. An inspection of Table 10 shows that this is clearly not the case. A positive value means that a component is produced, and a negative value means that it is consumed by the sum of the observed reactions.

Several reasons for the lack of mass balance have been considered:

(1) The grain-boundary phase may change composition by acting as a source or sink for the material required to balance the system. This seems implau-

sible, because it requires a grain-boundary phase which contains more than one-half percent of the cations in the rock, with a composition high in Fe, Mg, and K at the beginning of the process and becomes silica-rich as the reaction proceeds. Evidence for this much grain-boundary material is lacking in the rocks. In addition, the required composition of the grain-boundary phase is not at all like the reported compositions of fluid inclusions thought to represent the fluids during metamorphism.
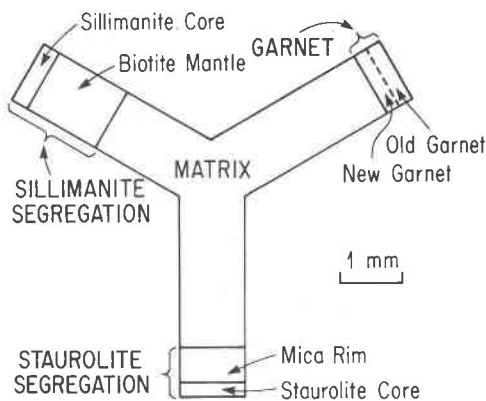
(2) The system is not closed on the scale of a thin section and communicates with other domains outside of the thin section. Metasomatism on a scale larger than an outcrop seems unlikely, because the only observed trend in bulk composition as a function of grade was dehydration. In addition, no metasomatic features such as extensive vein networks were noticed in the field. Exchange of material by diffusion between different domains within an outcrop seems to be ruled out, because if this was the case a component should be produced in some specimens and consumed in others from the same outcrop, so that the consumption and production balance out over the outcrop as a whole.

(3) There is an error in identifying the product and reactant regions or in measuring the amount of reaction that has occurred. This is not likely because it is possible to identify the reactants and products by observing the development of the segregations starting at the staurolite zone/lower sillimanite zone isograd and proceeding upgrade until the staurolite has completely disappeared. The general consistency in the sign and magnitude of the sums indicates that the random errors in the measurements of the amounts of product and reactant regions are not causing the observed excesses and deficits.

(4) Additional reactions occurring in the rock have not been taken into account in this analysis. Two types of reactions have not yet been considered:

(a) Incongruent reactions, where the mineral com-

Table 10. Cumulative mass transfer during growth of sillimanite segregations. Units are 10^{-4} moles/cm^3 of rock

Outcrop		MnO	FeO	ZnO	NaO$_{1/2}$	MgO	AlO$_{3/2}$	SiO$_2$	KO$_{1/2}$	CaO	TiO$_2$	H$_2$O
THROUGH THE BIOTITE MANTLE OF THE SILLIMANITE SEGREGATION												
RA66	Mean	0.002	0.679	0.000	0.070	0.437	−3.455	1.259	0.418	0.013	0.073	0.503
	σ*	±0.002	±0.387	±0.000	±0.053	±0.267	±1.967	±1.088	±0.261	±0.012	±0.075	±0.309
RA69	Mean	0.002	0.299	0.002	0.038	0.184	−1.989	1.038	0.176	0.007	0.030	0.216
	σ	±0.002	±0.056	±0.002	±0.025	±0.042	±0.262	±0.284	±0.030	±0.007	±0.010	±0.038
THROUGH THE MATRIX AROUND THE SILLIMANITE SEGREGATION												
RA66	Mean	−0.005	−0.940	0.002	0.671	−0.488	−3.754	2.283	1.024	0.096	−0.156	1.325
	σ	±0.003	±0.432	±0.002	±0.173	±0.432	±1.881	±1.909	±0.450	±0.048	±0.218	±0.540
RA69	Mean	−0.007	−2.024	0.007	0.795	−1.122	−2.738	2.540	1.278	0.061	−0.309	1.632
	σ	±0.005	±1.285	±0.012	±0.216	±0.752	±1.581	±3.840	±0.309	±0.063	±0.269	±0.402
THROUGH THE MATRIX AROUND GARNETS												
RA66	Mean	−0.153	−1.403	0.000	0.110	0.035	−0.322	0.923	0.360	−0.045	0.050	0.443
	σ	±0.045	±0.417	±0.000	±0.033	±0.040	±0.139	±0.400	±0.116	±0.017	±0.018	±0.143
RA69	Mean	−0.126	−1.174	0.002	0.088	0.023	−0.342	0.965	0.251	−0.040	0.037	0.314
	σ	±0.022	±0.279	±0.002	±0.007	±0.013	±0.066	±0.239	±0.060	±0.012	±0.012	±0.078
THROUGH THE MICA RIM OF THE STAUROLITE SEGREGATION												
RA66	Mean	0.017	1.184	0.098	−0.422	0.229	3.704	−0.586	−2.180	−0.005	−0.093	−1.489
	σ	±0.003	±0.565	±0.061	±0.143	±0.171	±0.880	±0.593	±0.619	±0.013	±0.158	±0.437
RA69	Mean	0.010	0.213	0.437	−0.462	−0.613	4.423	−0.523	−1.971	−0.003	−0.226	−1.283
	σ	±0.005	±0.128	±0.095	±0.075	±0.183	±1.089	±0.501	±0.408	±0.020	±0.146	±0.291
THROUGH THE MATRIX AROUND THE STAUROLITE SEGREGATION												
RA66	Mean	0.017	1.122	0.098	−0.425	−0.272	3.905	−0.785	−2.130	−0.010	−0.093	−1.423
	σ	±0.003	±0.491	±0.061	±0.133	±0.123	±0.983	±0.709	±0.606	±0.017	±0.158	±0.423
RA69	Mean	0.012	0.208	0.437	−0.443	−0.624	4.767	−1.084	−1.886	−0.005	−0.211	−1.169
	σ	±0.005	±0.093	±0.095	±0.095	±0.151	±0.958	±0.291	±0.422	±0.018	±0.131	±0.302
SUM OF MATRIX MASS TRANSFER												
RA66	Mean	−0.139	−1.220	0.100	0.355	−0.785	−0.171	2.419	−0.745	0.042	−0.199	0.345
	σ	±0.040	±0.339	±0.061	±0.151	±0.340	±1.126	±1.708	±0.327	±0.051	±0.264	±0.401
RA69	Mean	−0.121	−2.990	0.445	0.442	−1.723	1.687	2.421	−0.473	0.018	−0.483	0.777
	σ	±0.027	±1.501	±0.106	±0.227	±0.905	±0.905	±4.076	±0.438	±0.058	±0.242	±0.435

* σ is one standard deviation

position changes in response to the ability or inability of a component to be transported to or from other parts of the rock. A reaction of this type can be used to explain the ZnO excess in the sum of the mass transfer of ZnO. Staurolite analyses in the lower sillimanite zone show that ZnO content increases with grade. This suggests that the staurolite is dissolving incongruently, leaving zinc behind to be reincorporated in the remaining staurolite. Thus, the large calculated flux of zinc in the matrix surrounding the staurolite is artificial, due to the assumption that the staurolite dissolves congruently. A similar solution is available to explain the large MnO deficiency in the sum of the mass transfer of MnO in the rocks. Most of this occurs because the garnet/matrix reaction is a a large sink for MnO as the garnet grows. Analyses of garnet zoning in these rocks show that garnet rims in the middle and upper lower-sillimanite zone are Mn-poor relative to the core. This suggests that, as the garnet grows, MnO is not supplied from the rest of the rock in sufficient quantities to maintain a constant MnO concentration. Thus, the garnet rim becomes progressively poorer in Mn as it grows. Therefore, the MnO deficit shown in Table 10 is probably a result of the incorrect assumption that the garnet composition remains constant during the growth of the segregation.

(b) A reaction in the matrix region of the rock, either in response to chemical potential changes brought about by variations in P and T, or simply in small segregations which were overlooked. Some matrix reaction has obviously taken place, because there is usually at least 0.1 percent sillimanite in the matrix of the rocks in the middle and upper lower sillimanite zone which could not be assigned to a segregation large enough to map. This appears to be the most plausible explanation for most of the observed excess and deficit of mass, because the first three possibilities do not seem applicable in this situation, and incongruent solution or precipitation seems only important for ZnO and MnO.

To obtain the matrix reaction that would best balance the mass in the system, a least-squares fit of the matrix phases to the excess or deficit of the components was made, with the restriction that the amount of sillimanite in the reaction must equal the observed amount of sillimanite in the matrix. ZnO was excluded in this calculation because it appears to remain in the staurolite lattice. In addition, the system was left open to water.

The average of the results of this calculation for each specimen at each outcrop are given in Table 11. The consistency of this reaction from specimen to specimen, and the presence of small amounts of sil-

Table 11. Coefficients and residuals for the reaction to close the system to all components except H_2O

Sample	Biotite	Muscovite	Ilmenite	Plagioclase	Sillimanite	Quartz	H_2O
			STOICHIOMETRIC COEFFICIENTS Units are 10^{-4} moles/cm^3 of rock*.				
RA66 Mean	−0.42	−0.02	−0.05	0.50	0.42	3.01	1.23
σ	±0.20	±0.25	±0.13	±0.23	±0.32	±2.76	±0.45
RA69 Mean	−1.00	0.81	−0.15	0.28	0.18	4.33	1.15
σ	±0.50	±0.30	±0.08	±0.32	±0.05	±3.98	±0.32
			VOLUME COEFFICIENTS FOR SOLID PHASES Units are volume percent of total rock.				
RA66 Mean	−1.28	−0.08	0.03	0.49	0.21	0.68	
σ	±0.61	±0.74	±0.09	±0.24	±0.16	±0.62	
RA69 Mean	−3.07	2.42	−0.10	0.23	0.09	0.99	
σ	±1.53	±0.90	±0.05	±0.40	±0.02	±0.90	

| | RESIDUALS Units are 10^{-4} moles/cm^3 of rock. | | | | | | | | | |
	MnO	FeO	$NaO_{1/2}$	MgO	$AlO_{3/2}$	SiO_2	$KO_{1/2}$	CaO	TiO_2	H_2O
RA66 Mean	−0.134	0.022	0.008	−0.022	0.005	0.000	−0.020	−0.060	−0.033	0.000
σ	±0.038	±0.030	±0.053	±0.025	±0.035	±0.000	±0.110	±0.013	±0.040	±0.000
RA69 Mean	−0.111	0.022	−0.025	−0.005	0.023	0.000	−0.075	−0.037	−0.020	0.000
σ	±0.020	±0.010	±0.023	±0.008	±0.018	±0.000	±0.060	±0.008	±0.010	±0.000

* Sillimanite = Al_2SiO_5; Quartz = SiO_2. Formulas for other phases given in Tables 1 through 6.

limanite in the matrix, support the conclusion that a small amount of reaction in the matrix does take place to close the system. Inspection of the MnO residuals from this calculation reveals that they are consistently large negative values, suggesting that the depletion of Mn in the growing garnet rims is the probable cause for the observed deficit of MnO in the system. The modal changes of the phases in this reaction are very small and impossible to verify, with the exception of sillimanite, because it was not originally present in the matrix allowing the formation of trace amounts to be easily recognized. Hence, it is not clear if the reaction in Table 11 represents a single reaction in the matrix, or if it is the net reaction produced by the sum of several minor local reactions in the matrix.

Conclusions

The overall reaction which occurred in pelites from the lower sillimanite zone on Elephant Mountain was the sum of several reactions taking place in local domains in the rock. Each local reaction produced a distinct type of mineral segregation which grew larger as the overall reaction proceeded. The local reactions were not isochemical, requiring that mass transfer take place between the segregations. A quantitative examination of the mass transfer in the rocks has shown that all components were able to migrate from one segregation to another in a mean molar reference frame during metamorphism. In addition to the reactions forming the segregations, a small amount of reaction was required of the matrix phases surrounding the segregations to close the system to all components but water.

The reaction mechanism which forms sillimanite segregations is apparently quite widespread in sillimanite-bearing rocks, as shown by the common occurrence of sillimanite nodules with biotite rims (*e.g.* Chinner, 1961; Eugster, 1970; Harwood, 1973). The nucleation of sillimanite within biotite, followed by the growth of sillimanite core at the expense of biotite mantle and the growth of biotite mantle at the expense of muscovite-bearing matrix, may be a common mechanism that forms sillimanite nodules of this type, because the core and rim reactions have similar stoichiometric coefficients. This is the ideal situation for segregations to develop (Fisher, 1973).

Acknowledgments

References

Bence, A. E. and A. L. Albee (1968) Empirical correction factors for the electron microanalysis of silicates and oxides. *J. Geol.*, *76*, 382–403.

Brady, J. B. (1975) Reference frames and diffusion coefficients. *Am. J. Sci.*, *275*, 954–983.

Carmichael, D. M. (1969) On the mechanism of prograde metamorphic reactions in quartz-bearing pelitic rocks. *Contrib. Mineral. Petrol.*, *20*, 244–267.

Chinner, G. A. (1961) The origin of sillimanite in Glen Clova Angus. *J. Petrol.*, *2*, 312–323.

Draper, N. R. and H. Smith (1966) *Applied Regression Analysis.* John Wiley and Sons, New York.

Eugster, H. P. (1970) Thermal and ionic equilibria among muscovite, K-feldspar and aluminosilicate assemblages. *Fortschr. Mineral.*, *47*, 106–123.

Fisher, G. W. (1970) The application of ionic equilibria to metamorphic differentiation: an example. *Contrib. Mineral. Petrol.*, *29*, 91–103.

—— (1973) Nonequilibrium thermodynamics as a model for diffusion-controlled metamorphic processes. *Am. J. Sci.*, *273*, 897–924.

—— (1975) The thermodynamics of diffusion-controlled metamorphic processes. In A. R. Cooper and A. H. Heuer, Eds., *Mass Transport Phenomena in Ceramics*, 111–122. New York, Plenum.

Foster, C. T., Jr. (1975) *Diffusion Controlled Growth of Metamorphic Segregations in Sillimanite Grade Pelitic Rocks near Rangeley, Maine, U.S.A.* Ph.D. Thesis, The Johns Hopkins University, Baltimore, MD.

Griffen, D. T. and P. H. Ribbe (1973) The crystal chemistry of staurolite. *Am. J. Sci.*, *273A*, 479–495.

Guidotti, C. V. (1968) Prograde muscovite pseudomorphs after staurolite in the Rangeley-Oquossoc areas, Maine. *Am. Mineral.*, *53*, 1368–1376.

—— (1970a) The mineralogy and petrology of the transition from the lower to upper sillimanite zone in the Oquossoc area, Maine. *J. Petrol.*, *11*, 277–336.

—— (1970b) Metamorphic petrology, mineralogy, and polymetamorphism in a portion of N.W. Maine. In G. M. Boone, Ed., *1970 New England Intercoll., Geol. Conf., 62d Ann. Meet. Field Trip B-1.*

—— (1974) Transition from staurolite to sillimanite zone, Rangeley quadrangle, Maine. *Geol. Soc. Am. Bull.*, *85*, 475–490.

Harwood, D. S. (1973) Bedrock geology of the Cupsuptic and Arnold Pond quadrangles, west-central Maine. *U. S. Geol. Surv. Bull. 1346.*

Moench, R. H. (1966) Relation of S₂ schistosity to metamorphosed clastic dikes, Rangeley-Phillips area, Maine. *Geol. Soc. Am. Bull.*, *77*, 1449–1462.

—— (1970a) Premetamorphic down-to-basin faulting, folding,

and tectonic dewatering, Rangeley area, western Maine. *Geol. Soc. Am. Bull., 81,* 1463–1496.

—— (1970b) Evidence for premetamorphic faulting in the Rangeley quadrangle, western Maine. In G. M. Boone, Ed., *1970 New England Intercoll. Geol. Conf. 62d Ann. Meet. Field Trip D.*

—— (1971) Geologic map of the Rangeley and Phillips quadrangles, Franklin and Oxford Counties, Maine. *U. S. Geol. Surv.*

Misc. Geol. Invest. Map I-605.

Robie, R. A., P. M. Bethke, M. S. Toulmin and J. L. Edwards (1966) X-ray crystallographic data, densities and molar volumes of minerals. In S. P. Clark, Jr., Ed., *Handbook of Physical Constants,* Revised Edition. Geol. Soc. Am., New York, 29–73.